Scientia Iranica F (2012) 19 (6), 1984–1990

Sharif University of Technology

Scientia Iranica

Transactions F: Nanotechnology

www.sciencedirect.com

On the buckling behavior of single-walled silicon carbide nanotubes

R. Ansari [a], S. Rouhi [b,*], M. Aryayi [a], M. Mirnezhad [a]

[a] *Department of Mechanical Engineering, University of Guilan, Rasht, P.O. Box 3756, Iran*

[b] *Department of Mechanical Engineering, Langroud Branch, Islamic Azad University, Langroud, Iran*

Received 2 February 2012; revised 3 May 2012; accepted 4 July 2012

KEYWORDS

Silicon carbide nanotubes;
Buckling;
Space frame model;
Density functional theory.

Abstract Silicon carbide nanotubes possess outstanding properties which enable them to have many applications. The buckling behaviour of silicon carbide nanotubes have been studied here. To do this, a 3D finite element method, known as space frame model has been proposed. Molecular mechanics are linked to density functional theory to derive the properties of this finite element method. It has been shown that the critical buckling force will diminish with increasing aspect ratio. Also, it is represented that increasing the aspect ratio will result in reducing the effect of boundary conditions.

1. Introduction

The outstanding properties of SiC including physical, chemical, and thermal properties enable it to be employed in high temperature, high frequency, and harsh environments [1]. There have been wide interests in nanostructures of SiC including nanotubes, nanowires and nanorods. The properties of these nanostructures are different from the bulk SiC [2]. There are some differences between silicon and carbon, for example, Si has lower electronegativity, weaker bonds (except when bonded to very electronegative atoms), kinetically more reactive, larger atomic radius, etc. These differences lead to differences in the properties of silicon compared with carbon [3].

Sun et al. [4] were the first ones who synthesized the silicon carbide nanotubes (SiCNTs) via the reaction of SiO with the multi-walled carbon nanotubes (MWCNTs). After the reaction, half of the carbon atoms of nanotubes were replaced by Si atoms. The interlayer distances of the resulting multi-walled silicon carbide nanotube (MWSiCNTs) were significantly larger than those of CNTs. It has been shown that there are two arrangements for SiC nanotubes. In type 1, the Si and C atoms are placed in alternating arrangement while each carbon atom has been bonded to three Si atoms and vice versa; however, in type 2 there are two Si and one C atoms are bonded to each C atom and vice versa. Ab initio studies on the stability of SiCNTs show that the nanotubes with the arrangement of type 1 are more stable than the other one [5].

Several theoretical methods have been employed to study the behaviour of nanotubes which can be categorized as atomistic and continuum mechanics approaches. The atomistic approaches can be classified as classical molecular dynamics (MD) [6,7], tight-binding molecular dynamics [8] and Density Functional Theory (DFT) [9]. The continuum mechanics approaches which are based on the principles of structural mechanics are classified as Bernoulli–Euler/Timoshenko beam models [10–12], shell models [13–15], and space frame models [16–21]. Employing the MD simulation method, Moon et al. [22] calculated the Young's modulus of SiC nanotubes. Bamieir et al. [23] used the ab initio method to study the elastic and electronic properties of SiC nanotubes. They also computed the strain energy and Young's modulus of nanotubes with different geometries.

Setoodeh et al. [24] utilized the MD simulation method to study the buckling behaviour of perfect and defective SiCNTs. They have represented that the effective Young's modulus of SiCNTs is weakly affected by the tube chirality and the tube diameter. They have also showed that the buckling forces of perfect nanotubes are more sensitive to temperature variation than defective nanotubes. Using the MD simulation combining with Tersoff potentials, Pan and Si [25] studied the response

* Corresponding author. Tel.: +98 1425244411; fax: +98 1425244422.
E-mail addresses: s_rouhi@iaul.ac.ir (R. Ansari), r_ansari@guilan.ac.ir (S. Rouhi), mirnezhad.mm@gmail.com (M. Aryayi), mahdiaryayi@gmail.com (M. Mirnezhad).

Peer review under responsibility of Sharif University of Technology.

Production and hosting by Elsevier

1026-3098 © 2012 Sharif University of Technology. Production and hosting by Elsevier B.V. Open access under CC BY-NC-ND license.
doi:10.1016/j.scient.2012.10.004

of single crystalline SiC nanotubes under tensile strain. They have indicated that at a constant wall-thickness, the mechanical properties are approximately independent of diameter of SiC nanotubes while the effect of wall-thickness on the mechanical properties is more important.

The atomistic methods, quantum mechanics and molecular dynamics, are very accurate, but they are very time consuming especially for large nanotubes. On the contrary, continuum models are computationally efficient and can be used for modeling large-sized systems at the nanometer scale. Thus, the need for developing a model including simultaneously the accuracy of the first category and the computational efficiency of the second category for mechanical analysis of nanotubes is greatly felt.

Herein, a 3D finite element model, known as space frame model, is developed to describe the buckling behavior of single-walled silicon carbide nanotubes (SWSiCNTs). Such a model relies on some information on the force constants of elements which are not available in the literature. These force constants are obtained here through equating the energy terms of molecular mechanics and quantum mechanics. Based on electronic structure of molecules calculations, quantum mechanics represents an accurate model. But, in spite of its accuracy, it is computationally expensive and time consuming even with exerting the simplifications. In molecular mechanics which is based on the Born–Oppenheimer approximation, the motion of electrons is ignored and system energy is described as a function of nucleus position. It is expected that this assumption, despite increasing the speed of solution, decreases the accuracy. So in the present paper, the molecular mechanics would be used combined with DFT to obtain the properties of the space frame model.

2. Molecular mechanics modeling

In molecular mechanics, the total potential energy can be expressed as combination of several energies due to bounded interactions or bounded and non-bounded interactions [26–29].

$$E_t = U_\rho + U_\omega + U_\tau + U_{vdw} + U_{es}, \tag{1}$$

in which $U_\rho, U_\theta, U_\omega$ and U_τ are energies associated with bond stretching, bond angle variation, bond inversion, and bond torsion, respectively; U_{vdw} and U_{es} are also associated with van der Waals and electrostatic interactions, respectively. Depending on material and loading conditions, these energy terms can be described by different energy functions. For SWNTs, it is expected that the main part of the potential energy system consists of U_ρ, U_θ and U_ω, and U_{vdw} can be neglected. Since Hook's law has been proved to be accurate and efficient in small deformations cases [28], it is used to describe the interaction between atoms in the system. Therefore, Eq. (1) can be rewritten as the following:

$$E_t = \sum \frac{1}{2} K_\rho (\Delta r)^2 + \sum \frac{1}{2} C_\theta (\Delta\theta)^2 + \sum \frac{1}{2} C_\omega (\Delta\phi)^2, \tag{2}$$

in which, as it has been represented in Figure 1., Δr, $\Delta\theta$ and $\Delta\phi$ are the bond elongation, bond angle variance and change of space between two atoms, respectively. The force constants of K_ρ, C_θ and C_ω which are respectively relevant to the stretching energy due to bond stretching, bond angle variation and bond inversion can be determined theoretically or experimentally. The average inversion angle ϕ can be computed as:

$$\phi = \frac{1}{3}(\beta_1 + \beta_2 + \beta_3). \tag{3}$$

The angles β_1, β_2 and β_3 have been shown in Figure 2. As it can be seen in Figure 3, each atom in a nanotube has three bond lengths and three bond angles, so Eq. (2) can be rewritten in more specific form as the following:

$$E_t = \sum_{ij} \frac{1}{2} K_\rho \sum_k (dr_{ijk})^2 + \sum_{ij} \frac{1}{2} C_\theta \sum_k (d\theta_{ijk})^2 + \sum_{ij} \frac{1}{2} C_\omega \left(\frac{1}{3} \sum_k (d\beta_{ijk}) \right)^2. \tag{4}$$

In addition, constant factor of $\frac{1}{2}$ in the first term of Eq. (4) indicates that the bond stretching energy is considered only once. The axial force of F associated with the chiral SWNTs can be decomposed into two components. The first one, f_p, is perpendicular to the bond r_3 and the other one, f_a is along the bond r_3 (see Figure 4). In the following, the geometrical relations of these two forces are expressed:

$$f_p = F \cos\left(\frac{\pi}{6} - \Theta\right), \tag{5}$$

$$f_p = F \sin\left(\frac{\pi}{6} - \Theta\right), \tag{6}$$

in which the chiral angle Θ is computed as:

$$\Theta = \arccos\left(\frac{2n+m}{2\sqrt{n^2+nm+m^2}}\right). \tag{7}$$

The considered coordinate system consists of two perpendicular axes; the first one is along the bond r_3 and the other one is perpendicular to it. This is because the length of the nanotube, which is considered infinite, consists of a repeatable cell. This cell is analyzed here. The force equilibrium equation can be written with respect to Figure 5 as:

$$f_p \sin\left(\frac{\theta_3}{2}\right) - f_a \cos\left(\frac{\theta_3}{2}\right) = K_\rho dr_1. \tag{8}$$

Also, the moment equilibrium leads to:

$$f_p \cos\left(\frac{\alpha}{2}\right)\left(\frac{r_1}{2}\right) = C_\theta d\theta_3 + C_\theta d\theta_2 \cos(\Psi), \tag{9}$$

where $C_\theta d\theta_3$ is rotation moment due to the bond angle variation in plane, $r_1 - r_2$, and $C_\theta d\theta_2 \cos(\Psi)$ is rotation moment induced by $d\theta_3$ in plane, $r_1 - r_3$. Via a protracted operation, Young's modulus and Poisson's ratio are attained as follows [30]:

$$Y = \frac{1}{2\pi Rt}\left(\frac{(n+m) K_\rho r_1}{\sin\left(\frac{\pi}{3}+\Theta\right)\sin\left(\frac{\theta_3}{2}\right)\left(\frac{\lambda_A K_\rho r_1^2}{C_\theta \tan^2\left(\frac{\theta_3}{2}\right)}+1\right)}\right), \tag{10}$$

$$v = -\frac{\cos\left(\frac{\theta_3}{2}\right)\left(1-\frac{\lambda_A K_\rho r_1^2}{C_\theta}\right)}{\left(1+\cos\left(\frac{\theta_3}{2}\right)\right)\left(\frac{\lambda_A K_\rho r_1^2}{C_\theta \tan^2\left(\frac{\theta_3}{2}\right)}+1\right)}. \tag{11}$$

The concept of surface Young's modulus is introduced here to keep away from defining the effective thickness. Surface Young's modulus can be defined as:

$$Y_s = Yt = \frac{1}{2\pi R}\left(\frac{(n+m) K_\rho r_1}{\sin\left(\frac{\pi}{3}+\Theta\right)\sin\left(\frac{\theta_3}{2}\right)\left(\frac{\lambda_A K_\rho r_1^2}{C_\theta \tan^2\left(\frac{\theta_3}{2}\right)}+1\right)}\right). \tag{12}$$

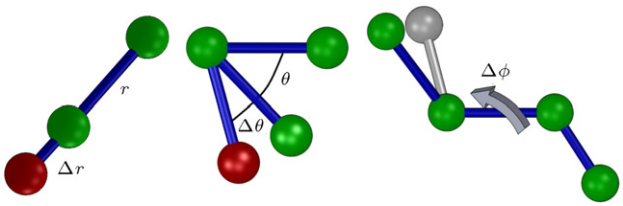

Figure 1: Different bonds structure of a SiC cell corresponding to each energy term.

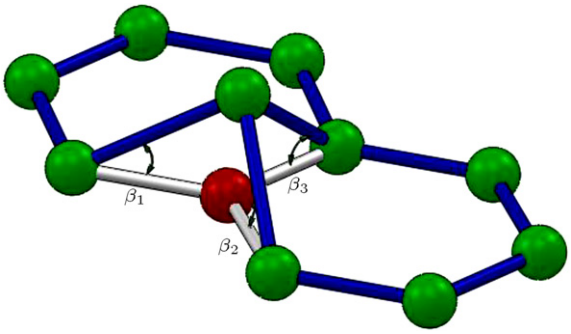

Figure 2: The components of average inversion angle ϕ.

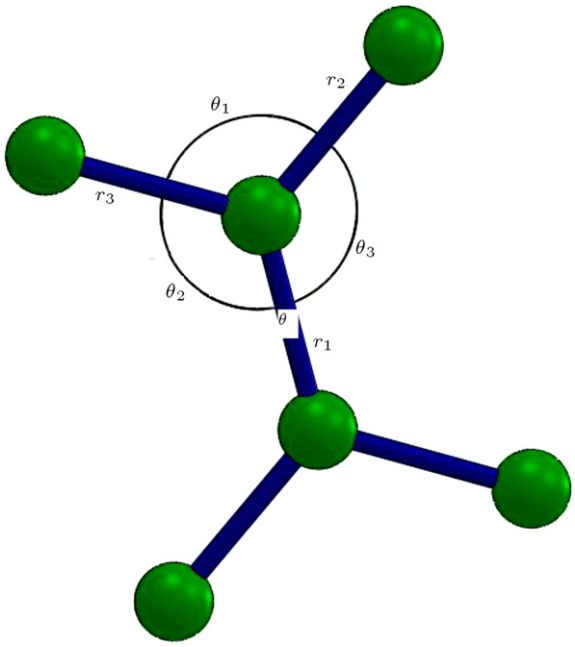

Figure 3: Different bonds and angles associated with an atom in nanotube structure.

3. Calculation of force constants

3.1. Mechanical properties of SiC using DFT

Based on the calculations of strain energy in the harmonic deformation range, elastic constants of SiC are computed here. By combining DFT [31,32] with Generalized Gradient Approximation (GGA) and Perdew–Burke–Ernzerhof (PBE) [33,34], these calculations would be performed. The Quantum–Espresso coding [35] is used to do all the above calculations.

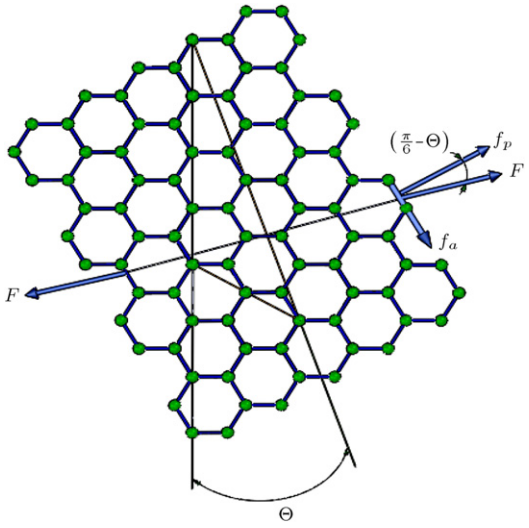

Figure 4: A (4, 2) chiral single-walled SiCNT subjected to axial load.

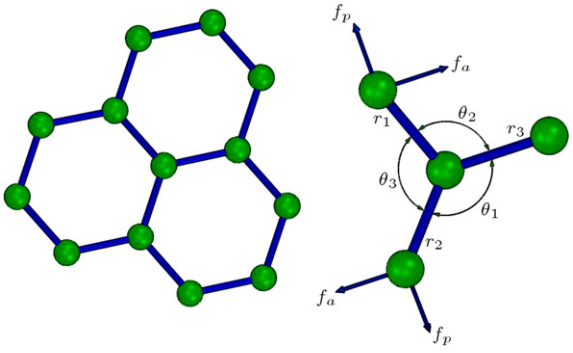

Figure 5: Schematic of a chiral single-walled SiCNT. (a) The hexagonal units, and (b) force distribution in bonds r_1 and r_2.

It has been reported that by increasing the dimension of the hexagonal unit cell, the results do not change substantially [36]. Therefore, the present work considers the smallest size of the unit cell for more simplicity [37]. Integration of Brillouin zone is accomplished with 20∗20∗1 Monkhorst and Pack k-point mesh. The SiC has a two-dimensional hexagonal unit cell, in which all atoms lie in the same plane. In this structure, the lattice constant and the bond length are computed, respectively, as $t = 3.093$ Ang and $d = 1.786$ Ang.

3.2. Young's modulus and Poisson's ratio

Due to the uncertainty in defining the thickness of nanotubes, surface Young's modulus is used here [36]:

$$Y_s = \left(\frac{1}{A_0}\right) \times \left(\frac{\partial^2 E_s}{\partial \varepsilon^2}\right), \tag{13}$$

in which A_0 represents the surface area in equilibrium, and E_s denotes the strain energy which can be computed using the following relation:

$$E_s = E_T(\varepsilon) - E_T(\varepsilon = 0), \tag{14}$$

in which $E_T(\varepsilon)$ is the total energy in the longitudinal strain ε and $E_T(\varepsilon = 0)$ represents the total energy at zero longitudinal

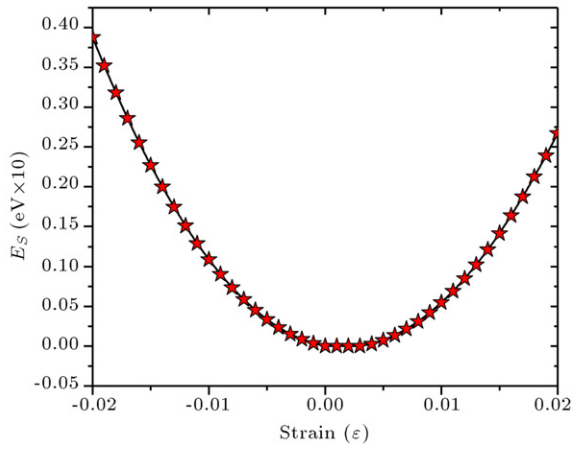

Figure 6: Variation of the strain energy E_s with strain for grapheme.

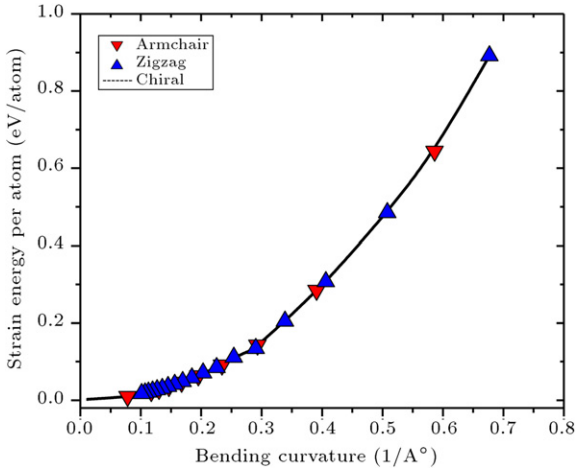

Figure 7: Strain energy relative to fully relaxed rolled planar SiC with varying radius plotted versus a quadratic approximation of the bending curvature with the flexural modulus predicted by the DFT.

strain. Moreover, the longitudinal strain can be formulated as $\varepsilon = \frac{\Delta t}{t}$, where t denotes the lattice constant. Poisson's ratio is defined as the ratio of transverse strain to longitudinal strain [36]:

$$v = -\frac{\varepsilon_{trans}}{\varepsilon_{axial}}. \tag{15}$$

As illustrated in Figure 6, the interval of $-0.02 < \varepsilon < 0.02$ can be considered as the harmonic area and after which a nonharmonic area will come in which higher order terms of the strain energy equation could not be neglected. Poisson's ratio and surface Young's modulus are obtained as 0.29 and 171 N/m, respectively.

The flexural rigidity is dependent on the strain energy of a 2D plane on its curvature in a desired direction:

$$D = \frac{\partial^2 E_f}{\partial K^2}, \tag{16}$$

in which $K\ (= 1/R)$ is the only curvature term of a single-layered structure which is not neglected [38,39] and E_f is the strain energy per atom which can be defined using the following expression:

$$E_f = E_n - E_{sh}, \tag{17}$$

where E_n and E_{sh} are the strain energy per atom of a fully relaxed rolled BN sheet and the strain energy per atom of a BN sheet, respectively. Figure 7 shows a representation of variation of E_f with respect to curvature. The strain energy relevant to the fully relaxed rolled SiC sheet with several radii is depicted as a quadratic approximate of bending energy and the flexural modulus is achieved utilizing DFT. The value of the flexural modulus computed is equal to 0.4407 ev(1.825 ev Ang/atom). Also, it should be mentioned that this value is independent of the rolling chirality. This means that these materials are isotropic.

3.3. Force constants

By substituting the values of $\theta_3 = \theta_2 = 2\pi/3$ and $n \to \infty$ into the Eqs. (11) and (12), the following relations are obtained [40]:

$$Y_s = \frac{8\sqrt{3}K_\rho}{\frac{K_\rho r_1^2}{C_\theta} + 18}, \tag{18}$$

$$v = \frac{\frac{K_\rho r_1^2}{C_\theta} - 6}{\frac{K_\rho r_1^2}{C_\theta} + 18}. \tag{19}$$

Substituting the values obtained for Young's modulus and Poisson's ratio into the above equations, the force coefficients are obtained as $K_\rho = 417.156$ nN/nm and $C_\theta = 0.842$ nN · nm. C_ω can be calculated by using the relation of $C_\omega = 24D$ [41], so $C_\omega = 1.505$ nN · nm.

4. Atomistic finite element modeling

Based on the analogy between graphene structures and macroscopic frame structures, a kind of finite element method, named as space frame model, is proposed in which bonds are simulated by beam elements. The elastic properties of beam elements can be computed as [16,17,20,21]:

$$d = 4\sqrt{\frac{C_\theta}{K_\rho}}, \qquad E = \frac{K_\rho^2 L}{4\pi C_\theta}, \qquad G = \frac{K_\rho^2 C_\omega L}{8\pi C_\theta^2}, \tag{20}$$

where d, E and G are diameter, Young's modulus and shear modulus of beams, and L is the beam length which is considered as bond length. Here, the bond length has been obtained as $L = 0.1786$ nm. By placing the computed force constants and length into Eq. (20), the elastic properties can be obtained as $d = 1.7971$ Ang, $E = 2.9372 \times 10^{-8}$ N/Ang^2 and $G = 2.6256 \times 10^{-8}$ N/Ang^2.

5. Results

Based on the above modeling procedure, the ANSYS commercial FE code was used to analyze the buckling behavior of SWSiCNTs. The axial force was applied uniformly at the nodes placed at one end. The geometry of nanotubes can be defined by the radius and length of it. The critical buckling force was obtained for different geometries. Table 1 shows the selected radii. The aspect ratio, length over radius, was chosen to be between 1 and 20. Also, the analysis was carried out for different boundary conditions including both ends clamped, both ends simply supported and clamped-free that simply named as clamed, simply supported and clamped-free boundary conditions.

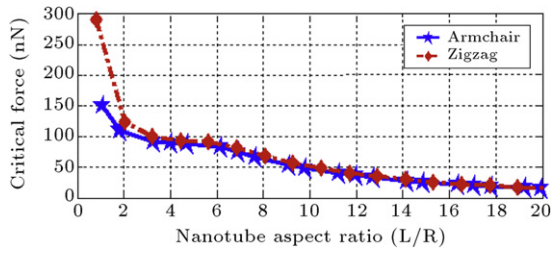

(a) Simply supported.

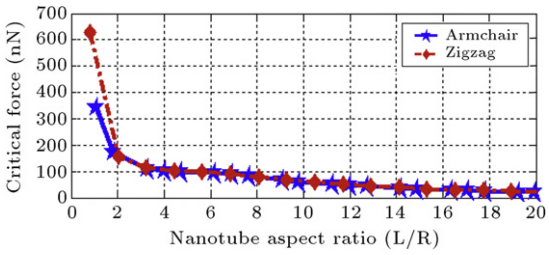

(b) Clamped.

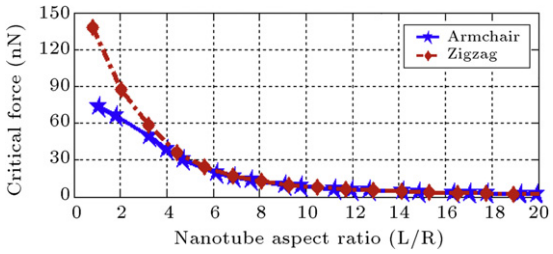

(c) Clamped-free.

Figure 8: Critical compressive forces of (a) simply supported, (b) clamped and (c) clamped-free nanotubes of radii $R = 4.26376$ Ang (armchair) and $R = 4.43103$ Ang (zigzag) versus nanotube aspect ratio.

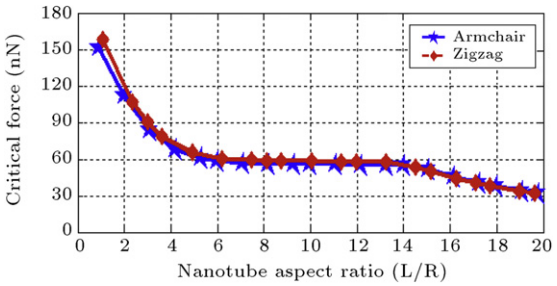

(a) Simply supported.

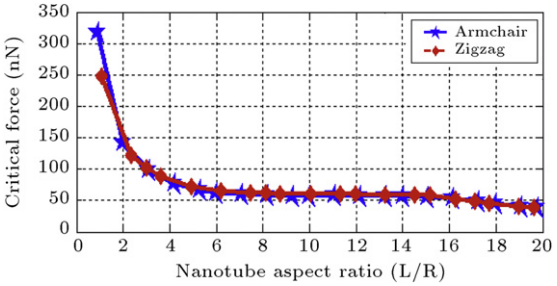

(b) Clamped.

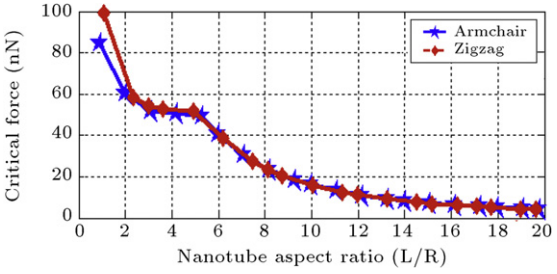

(c) Clamped-free.

Figure 9: Critical compressive forces of (a) simply supported, (b) clamped and (c) clamped-free nanotubes of radii $R = 8.52752$ Ang (armchair) and $R = 8.36972$ Ang (zigzag) versus nanotube aspect ratio.

The critical compressive force of armchair and zigzag nanotubes are drawn in Figures 8 and 9. From these figures, it can be seen that the critical buckling force will diminish with increasing aspect ratio. The slopes of curves are higher at first, but then they will reduce. It means that for long nanotubes, the sensitivity of SWCNTs to length will reduce. Also, it can be seen that the zigzag nanotubes are more stable than the armchair ones, when L/R is smaller than 4 (Figure 8) or 2 (Figure 9). The difference diminishes for long nanotubes so that increasing aspect ratio will lead to decreasing the effect of atomic structure. Comparing the graphs for two different radii reveals that at the same aspect ratios, the nanotubes with larger radii will buckle at smaller loads.

The effect of boundary conditions is represented in Figure 10. It can be seen that the critical buckling forces of nanotubes are the highest for clamped and the smallest for clamped-free boundary conditions. Also, it has been shown that the effect of boundary conditions will reduce for long nanotubes.

Table 1: Selected radii for nanotubes.

	Armchair	
Chirality	(5, 5)	(10, 10)
Radius (Ang)	4.26376	8.52752
	Zigzag	
Chirality	(9, 0)	(17, 0)
Radius (Ang)	4.43103	8.36972

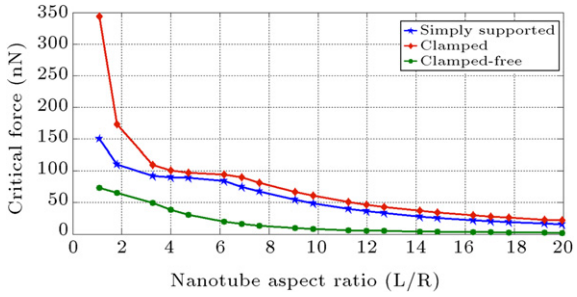

Figure 10: Critical compressive forces of an armchair nanotube with radius $R = 4.26376$ Ang versus nanotube aspect ratio under different boundary conditions.

6. Concluding remarks

The buckling behavior of SWSiCNTs has been analyzed here. To do this, a 3D finite element method model was developed in which bonds of graphene structures are modeled by beam and elements. To compute the properties of these beam elements, some force constants should be obtained. A combination of molecular mechanics and DFT was used to compute these force constants and by using them, the elastic properties of beam elements were derived. Having modeled the SWSiCNTs in this way, the critical compressive force of nanotubes was obtained for different geometries and boundary conditions. It was observed that by increasing the length of nanotubes, the critical compressive forces of nanotube will decrease. Also, it was shown that at a same side length, nanotubes with smaller radii are more stable. Having compared the critical compressive force for different boundary conditions, it was seen that increasing the aspect ratio will result in reducing the effect of boundary conditions.

References

[1] Fissel, A., Schröter, B. and Richter, W. "Low-temperature growth of SiC thin films on Si and 6H–SiC by solid-source molecular beam epitaxy", *Appl. Phys. Lett.*, 66(23), pp. 3182–3184 (1995).
[2] Dai, H., Wong, E.W., Lu, Y.Z., Fan, S. and Lieber, C.M. "Synthesis and characterization of carbide nanorods", *Nature*, 375, pp. 769–772 (1995).
[3] Teo, B.K., Huang, S.P., Zhang, R.Q. and Li, W.K. "Theoretical calculations of structures and properties of one-dimensional silicon-based nanomaterials: Particularities and peculiarities of silicon and silicon-containing nanowires and nanotubes", *Coord. Chem. Rev.*, 253(23–24), pp. 2935–2958 (2009).
[4] Sun, X.H., Li, C.P., Wong, W.K., Wong, N.B., Lee, C.S., Lee, S.T. and Teo, B.T. "Formation of silicon carbide nanotubes and nanowires via reaction of silicon (from disproportionation of silicon monoxide) with carbon nanotubes", *J. Am. Chem. Soc.*, 124(48), pp. 14464–14471 (2002).
[5] Menon, M., Richter, E., Mavrandonakis, A., Froudakis, G.E. and Andriotis, A.N. "Structure and stability of SiC nanotubes", *Phys. Rev. B.*, 69(11), p. 115322 (2004).
[6] Iijima, S., Brabec, C., Maiti, A. and Bernholc, J. "Structural flexibility of carbon nanotubes", *J. Chem. Phys.*, 104(5), pp. 2089–2092 (1996).
[7] Yakobson, B.I., Campbell, M.P., Brabec, C.J. and Bernholc, J. "High strain rate fracture and C-chain unraveling in carbon nanotubes", *Comput. Mater. Sci.*, 8(4), pp. 341–348 (1997).
[8] Hernandez, E., Goze, C., Bernier, P. and Rubio, A. "Elastic properties of C and $B_xC_yN_z$ composite nanotubes", *Phys. Rev. Lett.*, 80(20), pp. 4502–4505 (1998).
[9] Sanchez-Portal, D., Artacho, E., Soler, J.M., Rubio, A. and Ordejon, P. "Ab initio structural, elastic, and vibrational properties of carbon nanotubes", *Phys. Rev. B.*, 59(19), pp. 12678–12688 (1999).
[10] Zhang, Y.Q., Liu, X. and Zhao, J.H. "Influence of temperature change on column buckling of multiwalled carbon nanotubes", *Phys. Lett. A.*, 372(10), pp. 1676–1681 (2008).
[11] Zhang, Y.Y., Wang, C.M. and Tan, V.B.C. "Assessment of Timoshenko beam models for vibrational behavior of single-walled carbon nanotubes using molecular dynamics", *Adv. Appl. Math. Mech.*, 1(1), pp. 89–106 (2009).
[12] Lee, H.L. and Chang, W.J. "A closed-form solution for critical buckling temperature of a single-walled carbon nanotube", *Physica E*, 41(8), pp. 1492–1494 (2009).
[13] Ansari, R., Hemmatnezhad, M. and Ramezannezhad, H. "Application of HPM to the nonlinear vibrations of multiwalled carbon nanotubes", *Numerical Methods for Partial Differential Equations*, 26(2), pp. 490–500 (2010).
[14] Yakobson, B.I., Brabec, C.J. and Bernholc, J. "Nanomechanics of carbon tubes: Instabilities beyond linear response", *Phys. Rev. Lett.*, 76(14), pp. 2511–2514 (1996).
[15] Ru, C.Q. "Effective bending stiffness of carbon nanotubes", *Phys. Rev. B.*, 62(15), pp. 9973–9976 (2000).
[16] Li, C. and Chou, T.W. "A structural mechanics approach for the analysis of carbon nanotubes", *Int. J. Solid. Struct.*, 40(10), pp. 2487–2499 (2003).
[17] Tserpes, K.I. and Papanikos, P. "Finite element modeling of single-walled carbon nanotubes", *Composites B*, 36(5), pp. 68–477 (2005).
[18] Ansari, R., Rajabiehfard, R. and Arash, B. "Nonlocal finite element model for vibrations of embedded multi-layered graphene sheets", *Comput. Mater. Sci.*, 49(4), pp. 831–838 (2010).
[19] Arash, B. and Ansari, R. "Evaluation of nonlocal parameter in the vibrations of single-walled carbon nanotubes with initial strain", *Physica E*, 42(8), pp. 2058–2064 (2010).
[20] Ansari, R. and Rouhi, S. "Atomistic finite element model for axial buckling of single-walled carbon nanotubes", *Physica E*, 43(1), pp. 58–69 (2010).
[21] Rouhi, S. and Ansari, R. "Atomistic finite element model for axial buckling and vibration analysis of single-layered graphene sheets", *Physica E*, 44(4), pp. 764–772 (2012).
[22] Moon, W.H., Ham, J.K. and Hwang, H.J. "Mechanical properties of SiC nanotubes", Nanotechnology Conference and Trade Show, 3, Chapter 3: Carbon Nano Structures, pp. 158-161 (2003).
[23] Baumeier, B., Krüger, P. and Pollmann, J. "Structural, elastic, and electronic properties of SiC, BN, and BeO nanotubes", *Phys. Rev. B.*, 76(8), p. 085407 (2007).
[24] Setoodeh, A.R., Jahanshahi, M. and Attariani, H. "Atomistic simulations of the buckling behavior of perfect and defective silicon carbide nanotubes", *Comput. Mater. Sci.*, 47(2), pp. 388–397 (2009).
[25] Pan, H. and Si, X. "Molecular dynamics simulations of diameter dependence tensile behavior of silicon carbide nanotubes", *Physica B.*, 404(12-13), pp. 1809–1812 (2009).
[26] Allinger, N.L. "Conformational analysis 130. MM2. a hydrocarbon force field utilizing V1 and V2 torsional terms", *J. Am. Chem. Soc.*, 99(25), pp. 8127–8134 (1977).
[27] Burkert, U. and Allinger, N.L., *Molecular Mechanics*, American Chemical Society, Washington DC (1982).
[28] Leach, A.R., *Molecular Modelling Principles and Applications*, Addison Wesley Longman Limited, London 131–210 (1996).
[29] Odegard, G.M., Gates, T.S., Nicholson, L.M. and Wise, K.E. "Equivalent continuum modeling of nano-structured materials", *Compos. Sci. Technol.*, 62(14), pp. 1869–1880 (2002).
[30] Mirnezhad, M., Ansari, R. and Rouhi, H. "Effects of hydrogen adsorption on mechanical properties of chiral single-walled zinc oxide nanotubes", *J. Appl. Phys.*, 111(1), p. 014308 (2012).
[31] Szabo, A. and Ostlund, N.S., *Modern Quantum Chemistry*, McGraw-Hill, New York (1989).
[32] Hedin, L. "New method for calculating the one-particle Green's function with application to the electron-gas problem", *Phys. Rev. A.*, 139(3A), pp. 796–823 (1965).
[33] Perdew, J.P., Burke, K. and Ernzerhof, M. "Generalized gradient approximation made simple", *Phys. Rev. Lett.*, 77(18), pp. 3865–3868 (1996).
[34] Perdew, J.P., Burke, K. and Wang, Y. "Generalized gradient approximation for the exchange–correlation hole of a many-electron system", *Phys. Rev. B.*, 54(23), pp. 16533–16539 (1996).
[35] Giannozzi, P., Baroni, S., Bonini, N., Calandra, M., Car, R., Cavazzoni, C., Ceresoli, D., Chiarotti, G.L., Cococcioni, M., Dabo, I., Corso, A.D., de Gironcoli, S., Fabris, S., Fratesi, G., Gebauer, R., Gerstmann, U., Gougoussis, C., Kokalj, A., Lazzeri, M., Martin-Samos, L., Marzari, N., Mauri, F., Mazzarello, R., Paolini, S., Pasquarello, A., Paulatto, L., Sbraccia, C., Scandolo, S., Sclauzero, G., Seitsonen, A.P., Smogunov, A., Umari, P. and Wentzcovitch, R.M. "QUANTUM ESPRESSO: a modular and open-source software project for quantum simulations of materials", *J. Phys. Condens. Matter.*, 21(39), p. 395502 (2009).

[36] Topsakal, M., Cahangirov, S. and Ciraci, S. "The response of mechanical and electronic properties of graphane to the elastic strain", *Appl. Phys. Lett.*, 96(9), p. 091912 (2010).
[37] Monkhorst, H.J. and Pack, J.D. "Special points for Brillouin-zone integrations", *Phys. Rev. B.*, 13(12), pp. 5188–5192 (1976).
[38] Arroyo, M. and Belytschko, T. "Finite crystal elasticity of carbon nanotubes based on the exponential Cauchy–Born rule", *Phys. Rev. B*, 69(11), p. 115415 (2004).
[39] Lu, Q., Arroyo, M. and Huang, R. "Elastic bending modulus of monolayer graphene", *J. Phys. D: Appl. Phys.*, 42(10), p. 102002 (2009).
[40] Chang, T. and Gao, H. "Size-dependent elastic properties of a single-walled carbon nanotube via a molecular mechanics model", *Mech. Phys. Solids*, 51(6), pp. 1059–1074 (2003).
[41] Chang, T., Li, G. and Guo, X. "Elastic axial buckling of carbon nanotubes via a molecular mechanics model", *Carbon*, 43(2), pp. 287–294 (2005).

Reza Ansari received his Ph.D. from University of Guilan, Iran, in 2008. During his Ph.D. program, he was also a visiting fellow at Wollongong University, Australia in 2006–2007. He is currently a Faculty member at the Department of Mechanical Engineering, University of Guilan. He authored more than 60 refereed journal papers and 12 book chapters. His research background and interests include computational nano- and micro-mechanics, advanced numerical techniques, nonlinear analyses, prediction of mechanical behavior of smart composite/FGM shell-type structures.

Saeed Rouhi received his B.Sc. degree in mechanical engineering from University of Guilan, Iran, in 2006. He then received his M.S. degree with honors from University of Guilan in 2009. He is currently working as a lecturer in Islamic Azad University, Langroud Branch. His fields of interest are nanomechanoics, nanocomposites and mechanical behavior of structures including buckling and vibration.

Mahdi Aryayi received his B.S. degree in mechanical engineering from University of Guilan, Iran, in 2009. He then received his M.S. degree from University of Science and Technology 2012 with honors. His fields of interest are continuum modeling and mechanical behavior of nanostructures.

Mahdi Mirnezhad received his B.Sc. degree in mechanical engineering from Ferdowsy University of Mashhad, Iran, in 2008. He then received his M.Sc. degree from University of Guilan in 2011 with honors. His fields of interest are quantum mechanics, molecular mechanics and mechanical properties of nanostructures.